ISSN 2347 - 3983
Volume 9. No. 6, June 2021
International Journal of Emerging Trends in Engineering Research
Available Online at http://www.warse.org/IJETER/static/pdf/file/ijeter16962021.pdf
https://doi.org/10.30534/ijeter/2021/16962021

3D Numerical Modeling of Pile embankment performance on Soft Soil

Abdul Salam Brohi[1], Abdullah Saand[2], Zeeshan Ahmed Sahito[3]
[1]Department of Civil Engineering,
Quaid-e-Awam University of Engineering, Science & Technology, Nawabshah, Pakistan,
[1]eng.armaan@gmail.com , [2]abdullah@quest.edu.pk , [3]zeeshansahito5@gmail.com

ABSTRACT

Embankments are often required in many civil engineering construction projects involving infrastructure development to elevate the ground level. Due to the limitation of land availability for infrastructure projects in many countries, a large number of projects are now being carried out on soft ground. However, embankment construction over soft ground is a challenging task due to several undesirable characteristics associated with soft soils such as local instability, inadequate bearing capacity and large settlements, which can occur over a long period of time. These problems can generally result in expensive remedial measures and long construction delays. The conventional soft ground improvement methods based on consolidation such as vertical drains and preloading are not suitable when projects have to be completed within a short period of time or the ground improvement has to be carried out in contaminated ground. In such situations, reinforced pile-supported embankments are increasingly used as an alternative construction method due to the shorter construction time required compared to consolidation based methods and due to the higher reliability of the method when the subsoil properties cannot be relied upon. . This paper presents a comprehensive numerical study carried out using the finite element method in order to investigate the performance of reinforced pile supported embankment. A detailed parametric study is presented in three-dimensional conditions incorporating the full geometry of embankment system. The influence of pile embedded length, pile diameter, elastic modulus of piles, height of the embankment, construction rate of the embankment were investigated on the performance of the selected embankment.

Key words: piled embankment; soil reinforcement; load transfer, ground improvement

1. INTRODUCTION

Embankments are used frequently in civil engineering construction works, whenever there is a need to elevate the ground surface. This may be for construction of highways, railways or dams. When embankments are constructed on firm ground with good geotechnical characteristics, there will not be many difficulties due to compressibility and shear strength. However if they are built on soft ground, this may be the reverse. Due to the unavailability of proper land for construction, many projects are currently being undertaken on soft grounds, which were previously considered unsuitable [1]. Over the past few decades construction on soft ground has increased drastically due to the lack of suitable land. This is because of the rapid growth of the world population and resulting need of infrastructure development. Therefore, construction activities around river estuaries, marshy lands and coastal areas have now increased and these lands cannot be neglected as unsuitable for construction anymore [2] Earth structures and embankments supported by piles have been successfully applied for many projects especially for road construction. The piles act as a reinforcement of the soil in order to increase the bearing capacity of soft soil [3]. Numerous studies have already been conducted on reinforced piled earth structures. Model tests have been carried out. Furthermore different numerical investigations have already been performed. When shear strength and stiffness gain due to consolidation is unpredictable and availability of land is insufficient to change the embankment geometry, the most reliable and convenient solution among these techniques is the use of pile supports to carry the embankment load. Column supports can be hard columns such as piles (Jenck et al. and Han et al.[4-5]. The settlements in the foundation soil layer can be reduced. Pile supports are effective in difficult or extremely poor ground conditions such as landfills, Brownfield sites and dumps where engineering behaviour of soils are not well known and extracting soil properties by means of routine laboratory tests is difficult. In these situations, since majority of the embankment load is transferred to the piles [9]. According to Jung et al. [6] soft soils are categorized as soils having an unconfined compressive strength between 25 - 50 kPa and very soft clays are the soils with undrained compressive strength less than 25 kPa. So, this method is suitable for such soft soils and when the soil strength is reducing this method becomes more suitable the reinforcement provides lateral restraint and effectively increases the bearing capacity of the subsoil. The aim is the improvement of the global performance of compressible soils, both in terms of settlement reduction and

increase of the load bearing capacity. Among the various available techniques, the improvement of soils by incorporating vertical stiff piles appears to be a particularly appropriate solution; the technique consists in driving a group of regularly spaced piles through a soft soil layer down to an underlying competent substratum. The surface load being thus transferred to this substratum by means of those reinforcing piles, which illustrates the case of a piled embankment.[10-16].

2. THREE-DIMENSIONAL COUPLED CONSOLIDATION ANALYSIS

The main objective of this study is to carry Three-dimensional finite element analysis to investigate the performance of pile supported embankment on soft soil and discuss the effects of adding pile supports to the embankment. Therefore, general embankment geometry was selected for the analysis with one foundation soil layer. The geometry of the selected embankment along a pile row in the longitudinal direction is shown in Fig. 1

Selected soil profile consists of one soil layer, The soil layer is a soft clay layer of 30 m thickness which is resting on bedrock.

The embankment spans in the longitudinal direction and has a crest width of 12 m and a base width of 30 m. The side slopes are 1:1 (Vertical:Horizontal). The total height of the embankment fill is 6 m. The embankment is supported by circular concrete piles having a diameter of 0.8 m. The centre to centre spacing of the piles is 7.5 m. Piles used here are end bearing piles which are supported by bedrock. The embankment is constructed in different stages (i.e. h = 2, 2 and 2 m).

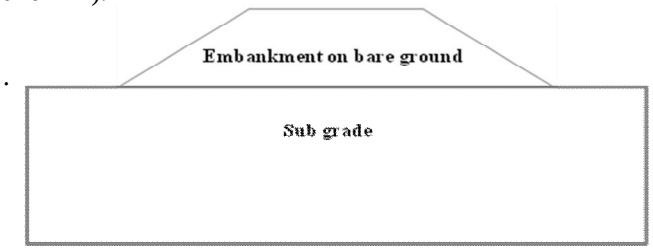

(a)

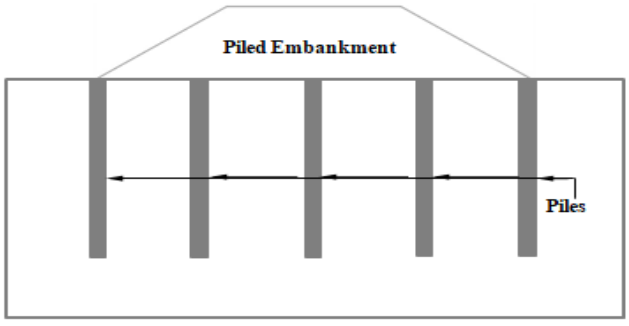

(b)

Fig.1. Configuration numerical run (a) elevation view (b) section view

2.1 FINITE ELEMENT MESH AND BOUNDARY CONDITIONS

Fig. 2 shows an isometric view of a finite element mesh used for analysing the embankment suppored on Piles .The size of the mesh for each numerical runs is 70 m × 8 m × 30 m. These dimensions were sufficiently large to minimise boundary effects in the numericalsimulation as further increment in the dimensions of the finite element mesh did not lead to any change in the computed results. Regarding the element size in the mesh, it is found that further halving the adopted mesh size only leads to a change of computed results of no more than 0.2%, suggesting the mesh is sufficiently fine. The piles-soil and embankment-soil interface was modelled as zero thickness by using duplicate nodes. The interface was modelled by the Coulomb friction law, in which the interface friction coefficient (μ) and limiting displacement (γ_{lim}) are required as input parameters.A limiting shear displacement of 5 mm was assumed to achieve full mobilization of the interface friction c. The interface was modelled by the Coulomb friction law, in which the interface friction coefficient (μ) and limiting displacement (γ_{lim}) are required as input parameters. A limiting shear displacement of 5 mm was assumed to achieve full mobilization of the interface friction equal to μ×p', where p' is the normal effective stress between two contact surfaces.

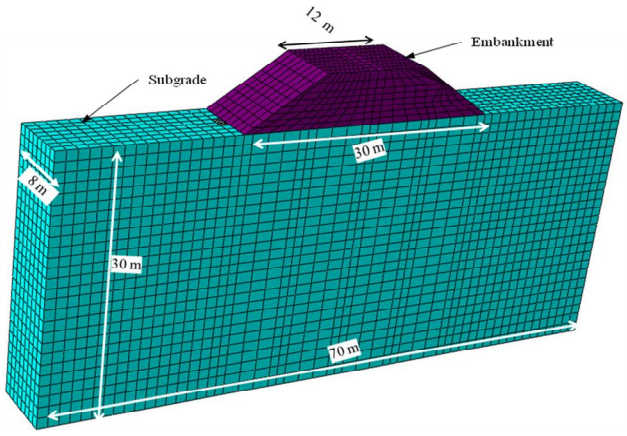

Fig.2. Finite element mesh

2.2 CONSTITUTIVE MODEL AND MODEL PARAMETERS USED IN FINITE ELEMENT ANALYSIS

2.3 CONSTITUTIVE MODEL

It is well recognized that to properly capture the ground deformation induced by unloading, it is vital to take into account the dramatic increase in soil stiffness upon reversal of stress path in the constitutive soil model. For this reason, an advanced hypoplastic clay model [21] coupled with the intergranular strain concept [22] was adopted in this numerical investigation to capture the nonlinear path-dependent soil stiffness at small strains. The constitutive model has been implemented in the commercial finite element software package Abaqus through a user-defined subroutine. The basic hypoplastic model was developed to

capture the nonlinear behaviour (upon monotonic loading at medium-to large-strain levels) of granular materials [21, 22]. The model allows for capturing different stiffness in loading, unloading, softening, hardening and the change of volume in shearing (i.e. dilation and compression). The current stiffness depends upon not only stress path but also recent stress history. In case of Hypoplastic clay model, the standard yield surface is replaced by boundary state surface. Hypoplastic model is generally described by a single nonlinear tensorial equation yielding the stress state $\dot{T}$ as a function of stretching rate D [21]. The general stress-strain relation is as follows:

$$\dot{T} = f_s\, L:D + f_s f_a\, N\|D\| \quad (1)$$

where L and N are fourth and second-order constitutive tensors, respectively. f_s and f_a are scalar factors expressing the influence of barotropy and pyknotropy.

The basic model consists of five parameters (N, λ*, κ*, φc and r) . The parameters N and λ* define the position and the slope of the isotropic normal compression line in the ln(1+e) versus ln p' plane. e is the void ratio, and p' is the mean effective stress. The parameter κ* defines the slope of the isotropic unloading line in the same plane. φc is the critical state friction angle, and the parameter r controls the large strain shear modulus. To account for the strain dependency and path dependency of the soil stiffness (at small strains), Niemunis and Herle [23] further improved the basic hypoplastic model by incorporating the concept of intergranular strain. The intergranular strain concept requires five additional parameters (R, β, χ, m_T and m_R) : R controls the size of the elastic range, and β and χ control the rate of stiffness degradation. The parameters m_T and m_R control the initial shear modulus upon 180° and 90° strain path reversal, respectively. In this hypothesised study, the parameters for silty clay were adopted Mašín et al., [21]. All the model parameters for silty clay reported by Wang et al., [24] are summarised in Table 1. The coefficient of lateral earth pressure at rest, Ko is estimated by Mayne and Kulhawy's [25] equation $K_o=(1-\sin\varphi)(OCR)^{\sin\varphi}$.

Table 1 Model parameters of kaolin clay adopted in the parametric study

Description	Parameter
Effective angle of shearing resistance at critical state: ϕ'	22°
Parameter controlling the slope of the isotropic normal compression line in the ln(1 + e) versus lnp plane, λ*	0.11
Parameter controlling the slope of the isotropic normal compression line in the ln(1 + e) versus lnp plane, κ*	0.026
Parameter controlling the position of the isotropic normal compression line in the ln(1 +e)–lnp plane, N	1.36
Parameter controlling the shear stiffness at medium- to large- strain levels, r	0.65
Parameter controlling initial shear modulus upon 180° strain path reversal, m_R	14
Parameter controlling initial shear modulus upon 90° strain path reversal, m_T	11
Size of elastic range, R	1×10^{-5}
Parameter controlling the rate of degradation of the stiffness with strain, β_r	0.1
Parameter controlling degradation rate of stiffness with strain, χ	0.7
Initial void ratio, e	1.05
Dry density (kg/m^3)	1136
Coefficient of permeability, k (m/s)	1×10^{-9}

2.4 NUMERICAL MODELLING PROCEDURE

The numerical analysis modelling procedure for a typical case is summarized as follows:

Step 1: Set up the initial boundary and initial effective stress conditions

Step2: Construct the embankment by activating the embankment elements.

3. RESULTS AND DISCUSSION

3.1 SETTLEMENT OF SUBGRADE DUE TO CONSTRUCTION OF EMBANKMENT

Fig. 3 compares the settlement of subgrade without and with piles due to construction of the embankment. For simplification, the subgrade without piles and with piles is referred as bare ground and piled embankment, respectively. The different construction stages of the embankment (h) are taken as 0.5, 1.0, 1.5, 2.0, 2.5, 3.0, 3.5, 4.0, 4.5, 5.0, 5.5 and 6.0 (i.e. 0.08, 0.16, 0.25, 0.33, 0.42, 0.50, 0.58, 0.67, 0.75, 0.83, 0.92 and 1.0). It can be seen from the figure that the settlement of the subgrade increases with construction of the embankment in the cases of bare ground and piled embankment. Initially, the settlement characteristics show the linear behaviour. However, as the embankment height increases beyond h/He=0.5, the rate of the settlement increased significantly. This is because of the self-weight of the embankment which induced larger shear strain in the ground. The shear strain results in the stiffness degradation of the subgrade ground. In this study, the ground (clay) is modelled using an advanced constitutive soil model (i.e. hypoplastic model) which is capable to capture stiffness degradation. As compared to the settlement of the bare ground, the settlement of the piled embankment is smaller. For the first four construction stages of the embankment, the settlement of the bare ground and piled embankment is similar. However, as the height of the embankment increases, the settlement of the piled embankment reduced significantly. This is because the piles provide stiffening effect in the ground. Moreover, piles transfer the load to deeper ground where the stiffness of the subgrade is higher than that of the

ground at shallower level. Owing to the stiffening effect of the piles and load transfer, the stiffness of the ground is increased substantially. Therefore, the settlement due to construction of the embankment reduced significantly. After completion of the embankment construction, the settlement of the piled embankment case reduced by 55% as compared to the bare ground case.

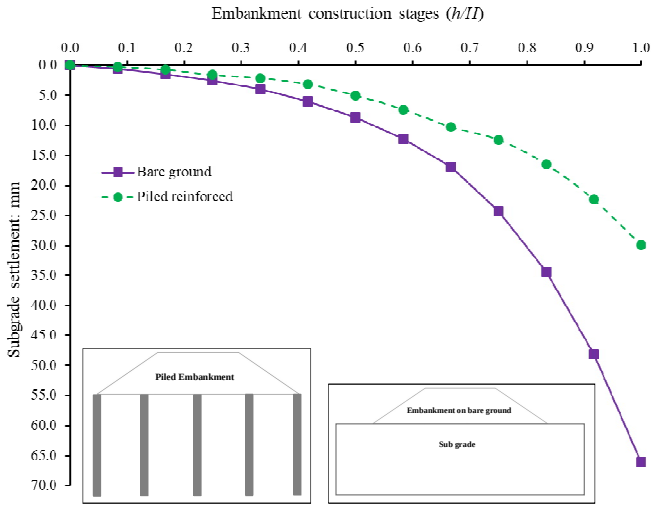

Fig: 3. Settlement of the subgrade during construction of embankment

3.2 *AXIAL LOAD DISTRIBUTION ALONG THE PILES LENGTH AFTER CONSTRUCTION THE EMBANKMENT*

In case of the piled embankment, six numbers of piles were installed (with centre to centre spacing of 7.5 m) along the cross section of the subgrade before construction of the embankment. Due to symmetry, three piles (i.e. P1, P2 and P3, see inset in Fig. 4) are selected to investigate load distribution along the pile. Fig. 4 shows the load distribution diagram along the lengths of piles P1, P2 and P3 after construction of the embankment. It can be seen from the figure that the pile installed in the middle of the subgrade section (i.e. Pile P3) has taken the largest load. On the hand, the load taken by the pile at the toe of the embankment (i.e. Pile P1) is the smallest load. This is because the height of the middle portion of the embankment is the maximum (i.e. 6 m). Since pile P3 has taken the largest load, the pile has mobilised shaft resistance along the length of the pile and end-bearing of the toe of the pile to support the load. On the contrary, negligible shaft resistance is mobilised along the length of pile P1. This is because of the smallest load is taken by pile P1. The average shaft resistance of magnitudes 27 kPa and 36 kPa is mobilised along pile P2 and pile P3, respectively. Pile P1 helps to reduce the heave of the subgrade at the toe of the embankment and hence subjected to significant lateral loading and bending moment. Because of the load transfer to the deeper ground through piles, the settlement of the piled embankment is smaller than that of the bare ground.

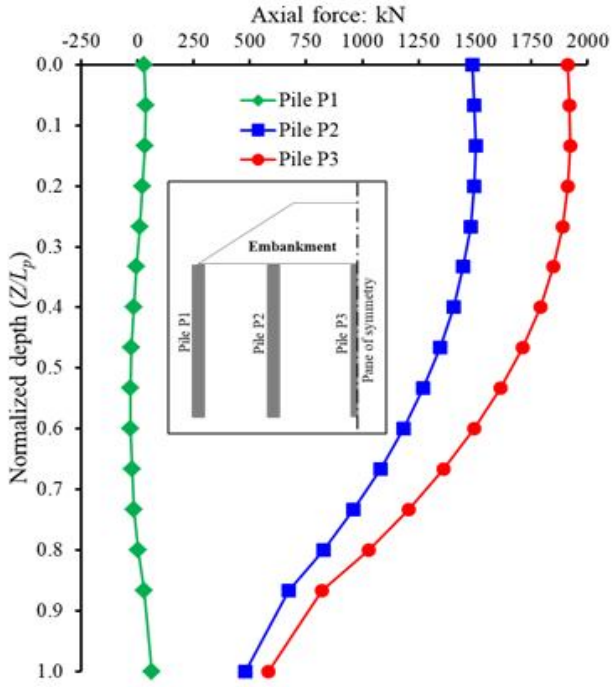

Fig: 4. Axial load distribution along pile length after embankment construction

3.3 *SHEAR FORCE DISTRIBUTION ALONG THE PILES LENGTH AFTER CONSTRUCTION THE EMBANKMENT*

In case of the piled embankment, six numbers of piles were installed (with centre to centre spacing of 7.5 m) along the cross section of the subgrade before construction of the embankment.

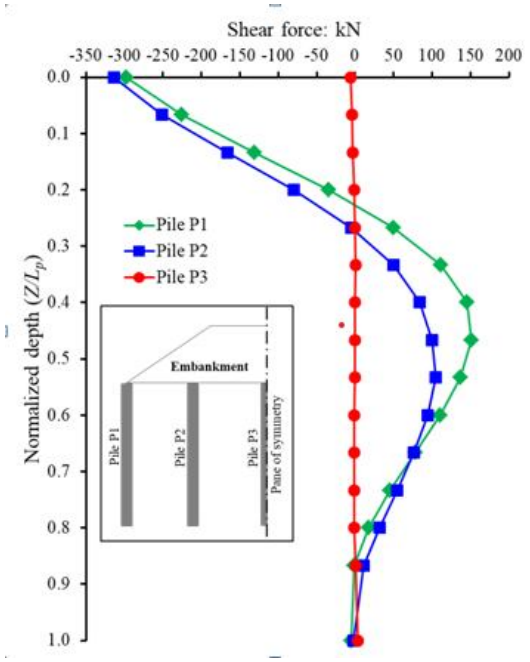

Fig. 5. Shear force distribution along pile length after embankment construction

Due to symmetry, three piles (i.e. P1, P2 and P3, see inset in Fig. 5) are selected to investigate lateral load (i.e. shear force) distribution along the pile. Fig. 5 shows the shear force distribution diagram along the lengths of piles P1, P2 and P3 after construction of the embankment. It can be seen from the figure that the pile installed at the toe of the embankment (i.e. Pile P1) and pile P2 is subjected to the largest lateral (negative) loading at the upper portion of the piles ($0 \leq Z/L_p \leq 0.2$). To balance the negative sharing force induce at the upper portion of the piles, the positive shearing is induced at the lower portion of both piles ($0.26 \leq Z/L_p \leq 0.80$). This is because the subgrade heaves at the toe of the embankment after the construction of the embankment. The lateral movement and heave is induced in the ground at the toe of the embankment due to construction of the embankment (discussed in section 3.5). On the contrary, the pile installed in the middle of the subgrade section (i.e. Pile P3) is subjected to negligible shear force along the shaft. This can ascribed to the subgrade ground movement on the completion of the embankment. Because the ground is only in vertical direction (i.e. downward), therefore no any shearing force was induced in pile P3. The maximum shear forces of 313 kN were induced at the heads of piles P1 and P2. From this study is revealed that all the six piles installed along the section of subgrade are useful to reduce the settlement of the embankment. The pile located in the middle of the embankment is supporting vertical load from the self-weight of the embankment and pile located at the toe of the embankment is resisting the lateral movement and heave in the subgrade due to construction of the embankment.

3.4 *BENDING MOMENT ALONG THE PILES LENGTH AFTER CONSTRUCTION THE EMBANKMENT*

As discussed in pervious section, the piles P1 and P2 are subjected to horizontal movement of subgrade induced due to construction of the embankment. Owing to the lateral movement of the ground, the piles are subjected to bending moment. Fig. 6 shows the induced bending profile along the lengths of piles P1, P2 and P3 after construction of the embankment. Because of the larger lateral movement of the subgrade near the toe of the embankment, larger bending moment is induced in pile P1 and pile P2. Since the head of piles are connected with the pile cap, positive bending moment was induced at the pile heads of pile P1 and pile P2. The maximum bending moment (negative) of 800 kNm was induced in pileP1 atZ/Lp=0.27. Because the ground is only in vertical direction (i.e. downward), therefore no any bending moment was induced in pile P3.No any bending moment was induced at the pile toes. This is because ground movement is at shallower depth of the subgrade. The piles are normally deigned to support vertical loading. However, while designing the piles for piled embankment, the piles should be designed to sustain lateral loading and bending moment.

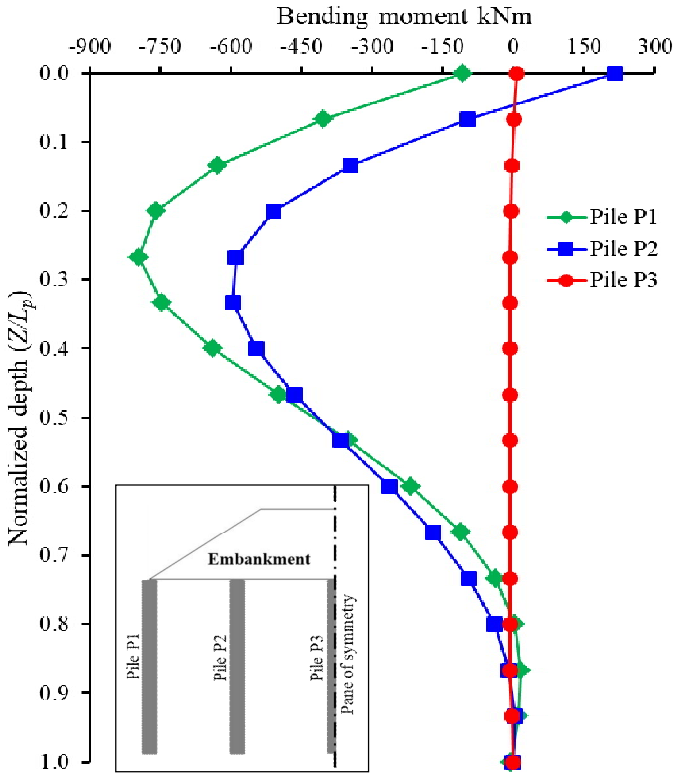

Fig. 6 Induced bending moment in piles

3.5 *INDUCED GROUND MOVEMENT AND DEVIATORIC STRAIN DUE TO CONSTRUCTION OF THE EMBANKMENT*

Figs.7(a) and (b) compare the subgrade ground movement and deviatoric strain generated after construction of the embankment in cases of bare ground and piled embankment. It can clearly be seen from the figure that soil movement at the middle of the embankment is in vertical direction (downward) in case of bare ground. On the other hand, the ground movement is in lateral direction at the toe of the embankment. Hence, the larger deviatoric strain is induced at the toe of the embankment. Owing to larger ground movement and deviatoric strain, the settlement of embankment was larger in case of bare ground. The maximum deviatoric strain of 10.5% is induced at the toe of the embankment. As compared to the induced ground movement and deviatoric strain in the subgrade of bare ground case, the ground movement and deviatoric strain are smaller in the subgrade of the piled embayment. This is because; the piles installed in the subgrade before construction of the embankment provide stiffening effect in the ground and transfer the load in the deeper layer of the subgrade. The improvement in the stiffness of the subgrade due to installation of the piles reduced the settlement of the embankment. The maximum deviatoric stain induced in case of piled embankment is 4.0%.

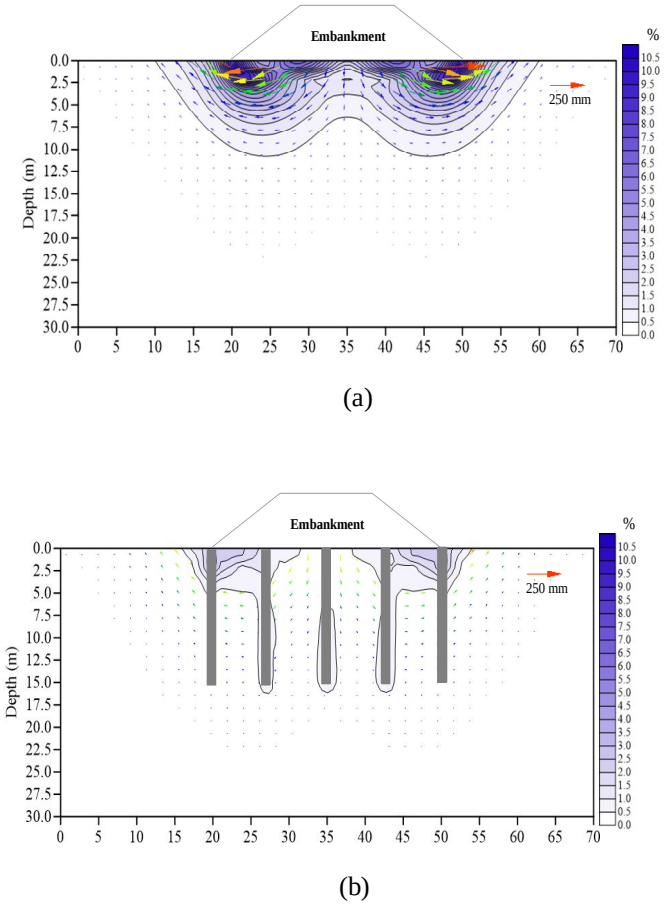

Fig: 7. Subgrade ground movement and deviatoric strain generated after construction of the embankment (a) bare case (b) piled embankment

3.6 *EFFECTS OF DIFFERENT DIAMETER AND EMBEDDED LENGTH OF PILES*

3.6.1 Settlement of the embankment

Fig. 8(a) compares the settlement of piled embankment with different pile diameters. For reference, the settlement of the embankment constructed on bare ground is included in the figure. It can be seen from the figure that the induced settlement of the piled embankment reduced with increment of the pile diameter. This is because the larger pile diameter pile carry larger load than that of piles with smaller diameter. The larger pile diameter provides higher stiffening effect in the subgrade and hence the settlement of the piled embankment reduced significantly. Comparing to the settlement of the pile embankment with pile diameter of 0.5 m, the settlement reduced by 24% in case of the pile embankment with pile diameter of 1.2 m. Fig. 8(b) compares the settlement of piled embankment with different embedded lengths. For reference, the settlement of the embankment constructed on bare ground is also included in the figure. It can be seen from the figure that the induced settlement of the piled embankment reduced with increment of the embedded length of the piles. This is because the deeper embedded pile diameter pile carry larger load than that of piles with smaller length. The deeper pile length transfers the load to the deeper layer of the subgrade and provides higher stiffening effect in the subgrade and hence the settlement of the piled embankment reduced significantly. Comparing to the settlement of the pile embankment with embedded length of 12 m, the settlement reduced by 50% in case of the pile embankment with embedded length of 21 m.

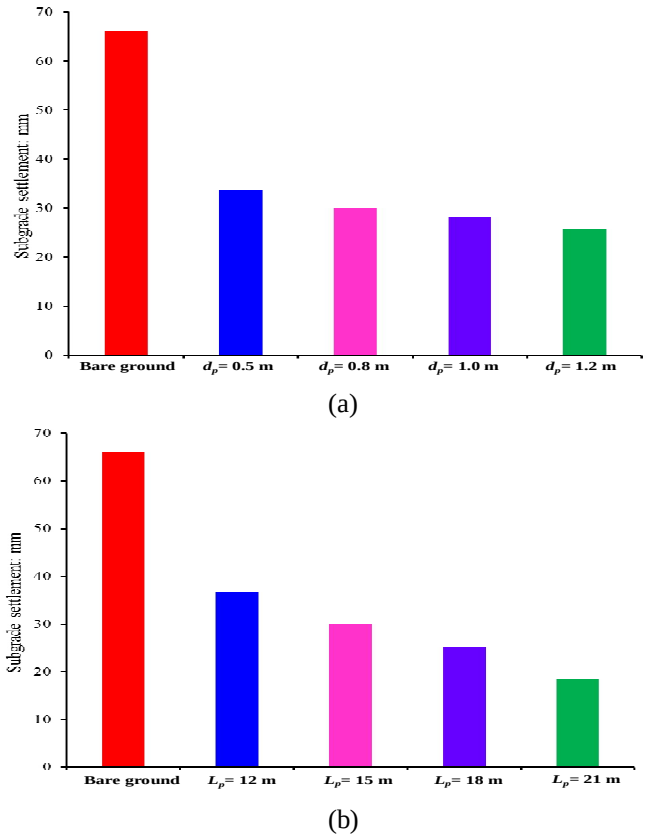

Fig.8. Settlement of piled embankment with (a) different pile diameters (b) different pile embedded lengths

4 SUMMARY AND CONCLUSIONS

The settlement of the subgrade increases with construction of the embankment in the cases of bare ground and piled embankment. As compared to the settlement of the bare ground, the settlement of the piled embankment is smaller. For the first four construction stages of the embankment, the settlement of the bare ground and piled embankment is similar. However, as the height of the embankment increases, the settlement of the piled embankment reduced significantly. After completion of the embankment construction, the settlement of the piled embankment case reduced by 55% as compared to the bare ground case.

(a). The pile installed in the middle of the subgrade section (i.e. Pile P3) has taken the largest load. On the hand, the load taken by the pile at the toe of the embankment (i.e. Pile P1) is the smallest load. Because of the load transfer to the deeper ground through piles, the settlement of the piled embankment is smaller than that of the bare ground.

(b). The pile installed at the toe of the embankment (i.e. Pile P1) and pile P2 is subjected to the largest lateral (negative)

loading at the upper portion of the piles ($0 \leq Z/L_p \leq 0.2$). To balance the negative sharing force induce at the upper portion of the piles, the positive shearing is induced at the lower portion of both piles ($0.26 \leq Z/L_p \leq 0.80$). It is revealed that all the six piles installed along the section of subgrade are useful to reduce the settlement of the embankment.

(c). Because of the larger lateral movement of the subgrade near the toe of the embankment, larger bending moment is induced in pile P1 and pile P2. Since the head of piles are connected with the pile cap, positive bending moment was induced at the pile heads of pile P1 and pile P2. The maximum bending moment (negative) of 800 kNm was induced in pileP1 at Z/L_p=0.27. Because the ground is only in vertical direction (i.e. downward), therefore no any bending moment was induced in pile P3.

(d). Soil movement at the middle of the embankment is in vertical direction (downward) in case of bare ground. On the other hand, the ground movement is in lateral direction at the toe of the embankment. Hence, the larger deviatoric strain is induced at the toe of the embankment. Owing to larger ground movement and deviatoric strain, the settlement of embankment was larger in case of bare ground. As compared to the induced ground movement and deviatoric strain in the subgrade of bare ground case, the ground movement and deviatoric strain are smaller in the subgrade of the piled embankment.

(e). With increment of pile diameter, the settlement of the embankment decreased. On the contrary, induced bending moment and shear force decreased.

(f). With increment of embedded length of pile, the settlement of the embankment induced bending moment and shear force decreased.

REFERENCES

[1]. Zhang, Z.; Rao, F.; Ye, G.: Design method for calculating settlement of stiffened deep mixed column-supported embankment over soft clay. Acta Geotech. 15(4), 795–814 (2019, 2020)

[2]. Rui, R.; Han, J.; Van Eekelen, S.J.M., et al.: Experimental investigation of soil-arching development in unreinforced and geosynthetic-reinforced pile-supported embankments. J. Geotech. Geoenviron. Eng. 145(1), 04018103 (2019)

[3]. G. Heerten, L. Vollmert, O. Doygun, A. Herold, and R. K¨orlin. Geokunststoffbewehrte
Gr¨undungspolster ¨uber Pf¨ahlen - Analyse international gebr¨auchlicher Bemessungsverfahren und
Anwendungsempfehlungen. 2. Symposium Baugrundverbesserung in der Geotechnik, 13./14.
September 2012, TU Wien, 401-416. 2012

[4]. Jenck, O., Dias, D. and Kastner, R. (2009a). Three-dimensional numerical modelling of a piled embankment, International Journal of Geomechanics, Vol. 9(3), pp. 102-112.

[5]. Jenck, O., Dias, D. and Kastner, R. (2009b). Discrete element modelling of a granular platform supported by piles in soft soil – validation on a small scale model test and comparison to a numerical analysis in a continuum. Computers and Geotechnics, Vol. 36(6), pp. 917-927.

[6]. Jung, H.S., Cho, C.G. and Chun, B.S. (2010). The engineering properties of surface layer on very soft clay of the south coast of Korea, Proc. of 2nd International Symposium on cone penetration testing, California.

[7]. Moormann, C., Lehn, J. and Aschrafi, J. (2016) 'Design of reinforced piled earth structures under static and variable loads', in: GeoAmericas 2016 3rd Pan-American Conference on Geosynthetics, Miami, United States, April 2016

[8]. Zhuang, Y. and Wang, K. (2018) 'Finite element analysis on the dynamic behavior of soil arching effect in piled embankment', Transportation Geotechnics. Elsevier Ltd, 14, pp. 8–21.

[9]. Magnan, J. P. (1994) 'Methods to reduce the settlement of embankments on soft clay: a review', in; the proceedings of Vertical and Horizontal Deformations of Foundations and Embankments (Geotechnical Special Publication No. 40) 1(40), pp.77-91

[10]. Deb K, Mohapatra SR. Analysis of stone column-supported geosynthetic-reinforced embankments. Appl Math Model 2013;37(5):2943–60 26 (2): 164–174. https://doi.org /10.1016/j.geotexmem.2007.05.004.

[11]. Liu, L., Zheng, G. and Han, J. (2010). Numerical analysis of lateral behaviour of rigid piles to support embankments, Proc. GeoShanghai 2010 International Conference, pp. 99-106

[12]. Wang, W., Zhou, A., and Ling, H. (2009). "Field tests on composite deepmixing cement pile foundation under expressway embankment." Slope Stability, Retaining Walls, and Foundations: Selected Papers from the 2009 GeoHunan Int. Conf., ASCE, Reston, VA, 62–67

[13]. Sloan, J. A. 2011. "Column-supported embankments: Full-scale tests and design recommendations." Ph.D. thesis, Dept. of Civil and Environmental Engineering, Virginia Tech.

[14]. Rowe R.K. and Liu K.W. 2015. Three-dimensional finite element modelling of a full-scale geosynthetic-reinforced, pile-supported embankment. Canadian Geotechnical Journal, 52(12): 2041–2054.

[15]. Almeida, M.S.S., Magnani, H.O., Dias, D. and Deotti, L.O.G. (2011), "Behaviour of three test embankments taken to failure on soft clay", Soil Rock., 34(4), 389-404

[16]. C. Moormann and J. Aschrafi. Optimisation of reinforced piled earth structures and embankments.
10th International Conference on Geosynthetics, 21-26 September 2014, Berlin, Germany. Paper
no. 129. 2014.

[17]. U. S. Okyay, D. Dias, L. Thorel, and G. Rault. Centrifuge Modeling of a Pile-Supported Granular

Earth-Platform. Journal of Geotechnical and Geoenvironmental Engineering, 140(2):4013015, 2014.

[18]. Zhuang, Y. and Wang, K. (2018) 'Finite element analysis on the dynamic behavior of soil arching effect in piled embankment', Transportation Geotechnics. Elsevier Ltd, 14, pp. 8–21.

[19]. Nunez MA, Briançon L, Dias D. Analyses of a pile-supported embankment over soft clay: full-scale experiment, analytical and numerical approaches. Eng Geol 2013;153:53–67

[20]. Liu H, Kong G, Chu J, Ding X. Grouted gravel column-supported highway embankment over soft clay: case study. Can Geotech J 2015. http://dx.doi.org/ 10.1139/cgj-2014-0284.

[21].D. Mašín, "A hypoplastic constitutive model for clays." Int. J. Numer. Analyt. Meth. Geomech., Vol. 29, No. 4, pp. 311-336, 2005

[22]. D. Mašín, I. Herle, "State boundary surface of a hypoplastic model for clays." Computers and Geotechnics, Vol. 32, No. 6, pp. 400-410, 2005

[23]. A. Niemunis, I. Herle, "Hypoplastic model for cohesionless soils with elastic strain range." Mech. Cohesive-Frict. Mater., Vol. 2, pp. 279-299, 1997

[24]. Wang, LZ, Chen, KX, Hong. Y, Ng, CWW. Effect of consolidation on responses of a single pile subjected to lateral soil movement. Canadian Geotechnical Journal 2015; 52(6): 769-782

[25]. L. M. Zhang, A. M. Y. Ng, "Probabilistic limiting tolerable displacements for serviceability limit state design of foundations." Géotechnique, Vol. 55, No. 2, pp. 151-161, 2005